 DOI: 10.1002/masy.200750113

Study on the Effect of Uniaxial Elongational Flow on Polyamide Based Nanocomposites

Emilia Garofalo, Giovanna Maria Russo, Luciano Di Maio, Loredana Incarnato*

Summary: This work focuses on the study of uniaxial elongational flow and its effects on morphology and stiffness of polyamide-6 based nanocomposites prepared by melt compounding. The elongational flow characterization was realized by converging flow method and fiber spinning technique. During the haul-off tests, fibers of the neat polyamide-6 and the hybrids (at 3 and 6 wt% of silicate) were collected at different draw ratios. Mechanical properties of the produced fibers were investigated and correlated to their nanostructure through analytical techniques sensitive to different aspects of morphology, such as DSC and TEM analysis. Rheological results, obtained with a capillary rheometer, indicate that the shear viscosity decreases with the silicate loading, while the extentional viscosity increases. Moreover, the presence of the silicate in polymer matrix leads to enhancements of draw-down force and reduction of the breaking draw ratio. In hybrid fibers an enhanced degree of exfoliation of the filler was observed upon drawing. Moreover, DSC analyses suggest that the crystalline structure of the fibers is the result of two opposite effects: the presence of the silicate which stabilizes the γ form and the drawing which promotes the α crystal phase. The degree of silicate exfoliation and the amount of the different crystal phases strongly affect the tensile properties of the fibers.

Keywords: elongational flow; mechanical properties; morphology; nanocomposites; polyamide-6

Introduction

Polymer-clay nanocomposites represent an interesting topic in materials research because of their promising properties which can be obtained with very low filler content. As well known, the performances improvement of these composites is realized when clay particles are accurately dispersed in the polymer matrix. Many researches [1–3] have been devoted to the problem of producing intercalated or exfoliated structures by melt compounding, and to verify the obtained morphology of the nanocomposites. In this regard, melt rheology represents a powerful method to investigate the bulk nanostructure,[4–6] conversely to other experimetal techniques (X-ray diffraction of even TEM micrography) that probes a very small volume, which may or may not be representative of the global structure. The most part of studies on rheology of polymer-clay nanocomposites concerns dynamic shear measurements which are very sensitive to the morphological state of the nanocomposite melts.[6–8] The study of the processability at high shear rates of such materials is instead more limited even if it is a crucial aspect for the production of polymer nanocomposite on wide scale. In particular, in the case of film or fiber extrusion, the elongational flow is common and a better understanding of its effects on the degree of silicate exfoliation and orientation inside the polymer matrix is important to optimize the final nanostructure and set proper processing conditions.

Department of Chemical and Food Engineering, University of Salerno, Via Ponte don Melillo, 84084 Fisciano (SA), Italy
E-mail: egarofalo@unisa.it

It is worthy pointing out that, in the case of a semicrystalline matrix, the properties are affected not only by the final nanostructure but also by the different crystal forms possibly present. Therefore, a systematic analysis of the elongational flow in nanocomposites systems must concern the influence of the stretching on dispersion and orientation of silicate inside the polymer matrix as well as the development of the crystal structure of the polymer matrix.

The present work focuses on the study of uniaxial elongational flow and to its effect on morphology and tensile properties of polymer-layered silicate nanocomposites. In particular polyamide based nanocomposites, prepared by twin screw extrusion melt compounding, were investigated. The elongational flow characterization was realized by converging flow method and fiber spinning technique by making use of a capillary rheometer.

Fibers of the neat polyamide-6 and the hybrids (at 3 and 6 wt% of silicate) were collected at different draw ratios.

The structural changes of the layered silicate and crystalline regions of the fibers were investigated in response to uniaxial deformation imposed. Tensile modulus of the produced fibers were also investigated and correlated to their nanostructure through analytical techniques sensitive to different aspects of the hybrids morphology, such as DSC and TEM analysis.

Experimental Part

Materials

The materials used for the preparation of nanocomposites were the Cloisite 30B (C30B), a layered sodium montmorillonite organically modified by N, methyl-N, tallow-N, N′, 2-hydroxyethyl-ammoniumchloride (90meq/ 100g clay), having interlayer basal spacing $d_{001} = 18.5$ Å, and Polyamide-6 matrix ($M_n = 54200$, I.V. = 3.4dl/g).

Melt Processing

The polyamide-layered silicate nanocomposites (wt 3% and wt 6%) were prepared by melt compounding using a Haake twin-screw extruder having counter-rotating intermeshing cone-shaped screw with L = 300 mm. A temperature profile of 265-260–255-245 °C from hopper to die was imposed and a screw speed of 60 rpm was set. Prior to processing, the materials were dried in a vacuum oven at 90 °C for 18 hours to avoid bubble formation and polymer degradation during processing.

Elongational Flow Characterization

It was realized by converging flow method and fiber spinning technique by making use of a capillary rheometer (Rosand RH7, Bohlin Instruments). The measurements were performed using a 1 mm diameter capillary die (L/D = 15) at 250 °C. The converging flow model developed by Cogswell was used for determining the approximate extensional viscosity values. In the fiber spinning experiments, performed with the capillary rheometer, the polymer melt was extruded at a piston velocity of 5 mm/min and was drawn at different velocities until the filament breaks. In particular, fibers of the neat polyamide-6 and the hybrids (at 3 and 6 wt% of silicate) were collected at draw ratios ranging between 0 and 45. The processing conditions, and sample nomenclature used for the discussion of results are reported in Table 1.

Characterization Techniques

Thermal analyses were carried out using a Mettler Differential Scanning Calorimeter (DSC30) and performing the following thermal cycle: a first heating at 10 °C/min from 0 to 260 °C; an isotherm at 260 °C for 10 min to melt the residual crystals and remove the thermo-mechanical history; a cooling to 0 °C and a reheating to 260 °C at the same scan rate. Cristallinity degrees, X_c, of the different fibers were determined by the ratio of heat of fusion of the sample on heat of fusion of the purely crystalline polyamide-6, i.e., 240 J/g.[9]

Transmission electron microscopy (TEM) analysis was conducted using a Philips EM 208 with different magnification levels. The images were get on sections

Table 1.
Processing conditions and sample nomenclature.

wt% Cloisite 30B	Draw Ratio	Polyamide-6 based hybrid fibers
0	0	PA0
	4	PA4
	18	PA18
	45	PA45
3	0	3PA0
	4	3PA4
	18	3PA18
	45	3PA45
6	0	6PA0
	4	6PA4
	18	6PA18

located normal to the fiber axis, prepared by microtoming of ultra-thin specimens with a Leica Utracut UCT microtome.

Mechanical tests were carried out, according to ASTM standard D3379/75, by an Instron 4301. The fibres were tested with a grip distance of 40mm and a cross-head speed of 5mm/min to measure the Young's modulus.

Results and Discussion

The amount of silicate exfoliation achieved in polyamide-6 nanocomposites during the compounding by twin screw extruder was verified through rheological and TEM investigations, widely discussed in our previous works.[10–12] The most significant results pointed out a strong correlation between the viscoelastic behaviour of the hybrids and their nanostructure in solid state. In particular, at low shear rates, the addition of the silicate results in non-Newtonian behaviour and a significant enhancement in the complex viscosity more pronounced with the increasing of the degree of silicate exfoliation.[13,14]

In order to understand the potential processability of layered silicate nanocomposites, the steady shear response at high shear flow conditions was investigated with converging flow technique, realized in a capillary rheometer.

The converging flow technique consists in forcing the molten polymer through a capillary by means of a piston moving in a cylindrical reservoir and, being an extrusion method, is widely applicable in the polymer processing sector as many processes are based on extrusion. So, the testing conditions more closely match the conditions experienced in processing, and thus the data are likely to be more relevant. The basic principle behind converging flow measurements is that the pressure drop in a contraction flow is due to both the shear and extensional flow properties of the material.[15]

Figure 1-a shows the shear viscosities of the neat matrix and the nanocomposite pellets containing 3wt% and 6wt% of organoclay. It is possible to observe that at high shear rates the viscosity and the shear thinning behaviour of the nanocomposites are comparable with the unfilled polymer, with a slight trend in decreasing viscosities values with increasing the silicate loading. The difference of the flow curves of the samples can be emphasized when the viscosity data are reported in function of the shear stress (Figure 1-b). As increasing the silicate loading the viscosity values decrease and the shear thinning behaviour become more pronounced with respect to neat polymer. Such results suggest that, at high shear rates, the structural network formed in the hybrids is oriented in flow direction so that the processability of the system is not compromised, but even improved, by the presence of filler.

In order to investigate the extensional behaviour of the molten systems, the experimental data obtained from capillary rheometry measurements were elaborated in terms of steady extensional viscosities by applying the converging flow model developed by Cogswell,[16] relating the pressure drop and flow rate for a specified geometry and the shear flow behaviour.

The plots of extensional viscosity vs. extensional rate for the polyamide-6 and the 3wt% and the 6wt% nanocomposite systems are reported in Figure 2. Comparing the curves, it is possible to note that, at high extentional rates, the presence of the silicate causes increases of extensional

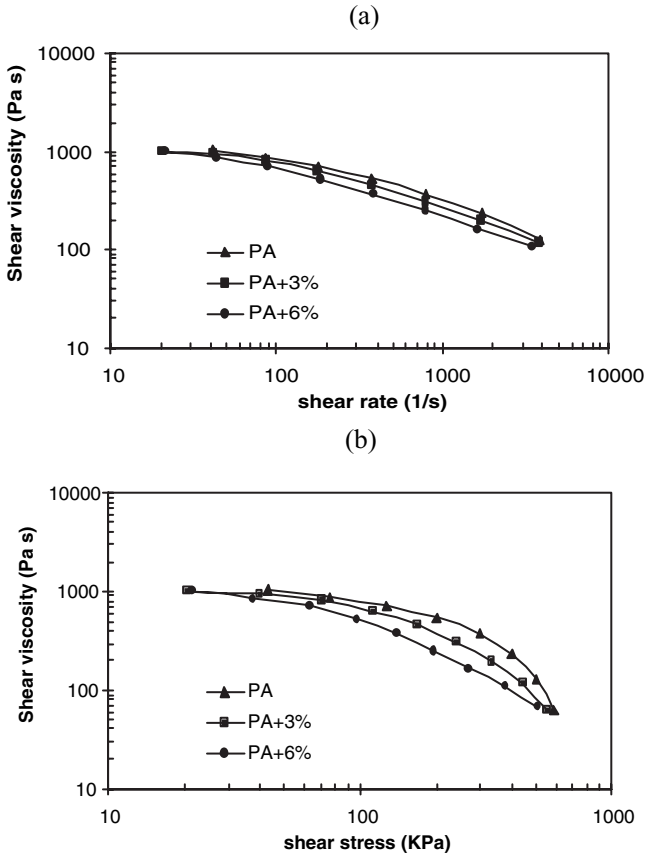

Figure 1.
Steady shear viscosity curves at 250 °C for the neat matrix and nanocomposite hybrids at 3 and 6 wt% of silicate loading: (a) steady shear viscosity in function of shear rate and (b) steady shear viscosity in function of shear stress.

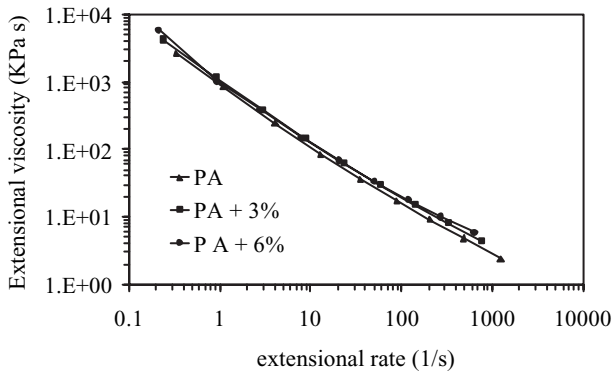

Figure 2.
Extensional viscosity curves at 250 °C for the neat matrix and nanocomposite hybrids at 3 and 6wt% of silicate loading.

viscosity, conversely to what happen to the shear viscosity above reported.

The increasing of extensional viscosity with the adding of the silicate can be related to behaviour of the dynamic storage modulus of the three systems, G′, reported in Figure 3. The monotonically increase of G′ values with the adding of silicate indicates enhanced elasticity of the nanocomposite with respect to the neat matrix. In particular, when the clay platelets are well dispersed in the polymer matrix, they build up a network-like structure due to their close interactions, which is also called a ''house of cards structure'' by Okamoto et al.[7] Friction between clay particle and polymer molecule and close inter-particle interactions hinder the uniaxial extensional flow of nanocomposite melts. The clay platelets act like branches of the macromolecular chain, which cause the increased viscosity values in extensional flow. Similar trend has been observed in highly long chain branched polyolefins.[17]

In order to investigate the effect of the uniaxial elongational flow on morphology and stiffness of the different systems, fibers at different draw ratios were produced by fiber spinning technique.

The extrudate filament at the exit of the capillary, cooled by exposure to ambient air, was drawn down by means of a motor-driven drum, and the tensile force in the filament was determined by measuring the vertical force on the rotating drum. So, the molten material firstly experiences a shear deformation in the capillary and then moves into a zone in which the deformation is primarily uniaxial extension. The test procedure (haul-off test) involves increasing the wind-up speed and recording the force level until the filament breaks.[15]

Figure 4 shows the force-extensibility diagram for the neat matrix and the 3 and 6wt% hybrids. It can be seen that the draw-down force of the samples increases with the silicate loading, while the breaking draw ratio decreases with the clay concentration. The increase of the haul-off force in presence of the silicate could be associated to the increased stiffness and elasticity of filled systems in turn attributed to the presence of well exfoliated regions and possible interactions between polymer chains and silicate layers. Moreover it is can be observed a strain hardening behaviour displayed by the neat matrix that is completely lost in the hybrid systems.

During the spinning tests, fibers of neat matrix and hybrids were collected at different draw ratios (DR = 0, 4, 18, 45) with the intention of study the effect of uniaxial drawing on morphology (silicate dispersion and exfoliation, orientation of the layered silicate and crystallites, matrix crystalline polymorphism) of nanocomposites.

In particular, the state of exfoliation and intercalation of silicate platelets inside polymer matrix was investigated by TEM analysis whereas information about the

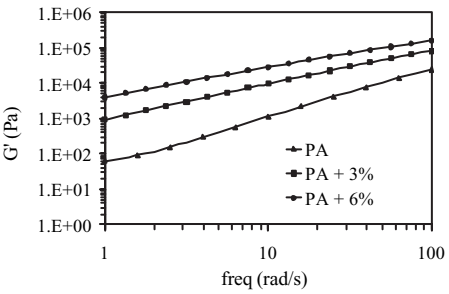

Figure 3.
Storage modulus plot for the neat matrix and nanocomposite hybrids at 3 and 6wt% of silicate loading obtained from oscillatory tests at 250 °C.

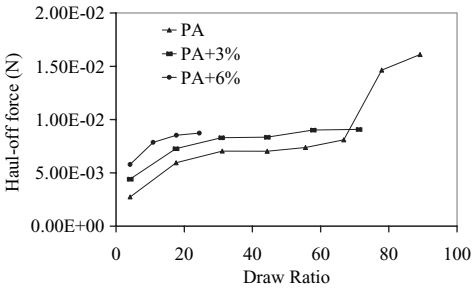

Figure 4.
Force-Extensibility diagram at 250 °C for the neat matrix and nanocomposite hybrids at 3 and 6wt% of silicate loading.

phase structure of hybrids was obtained by DSC analysis.

TEM images of nanocomposite samples with different clay amount and draw ratio were taken on sections normal to the stretching direction. The micrographs were captured with different magnification levels on the same normal section of the samples, in order to evidence the hierarchical structure of the hybrids. The low magnification images show the micron scale arrangement of primary clay particles in the PA matrix. Higher magnifications reveal a nano-scale dispersed morphology containing both individual silicate sheets and intercalated structures. Transmission electron micrographs of normal section of 3PA0 and 3PA18 were compared to the TEM image of the 3wt% nanocomposite sample as obtained by the melt compounding extrusion process (3PAextr). In Figure 5a-b the image corresponding to the 3PAextr nanocomposite clearly evidences that the silicate particles are distributed not uniformly in the polymer matrix: micron-scale morphology is comprised of dispersed primary particles and intercalated aggregates surrounded by a distribution of uncorrelated layers. On the other hand, the TEM micrograph of 3PA0 (Figure 6a–b) shows a significant change in the hybrid morphology: a more homogeneous dispersion of clay particles on micron-scale and a higher extent of silicate exfoliation on nano-scale with a macroscopic preferential orientation along the flow direction. This last result is probably a consequence of the shear deformation associated with the flow in the capillary. In fact, it should be considered that a fraction of polymer chains is chemically associated or hydrogen-bonded to the clay surface and, under the shear effect, the polymer chains may remain oriented and clay platelets can be aligned in the flow direction.[18,19]

Finally, the TEM micrograph (Figure 7a–b) of the 3wt% hybrid fiber at high draw ratio (3PA18) evidences a further increase of exfoliation of the silicate particles, while a slightly less extent of orientation is also observed. This is in agreement with the results of Pavlikovà et al.[20] who observed in layered silicate nanocomposite fibers an enhanced degree of exfoliation of the filler upon drawing. They also demonstrated that, during stretching, not all particles of clay orient themselves along fiber axis, but form self-assembled exfoliated structures. In particular, fiber obtained at higher draw ratio had a greater amount of self-assembled exfoliated structures. Moreover an increase of filler loading in the fibers also increases the content of self-assembled structures. These three-dimensional arrangements remind to the house of cards structure for layered clay nanocomposite melt under pure elongational flow.[7]

It is well known that nanofillers can also influence polyamide polymorphism,[10,21] characterized by an α-phase constituted by extended-chain sheet structure and a

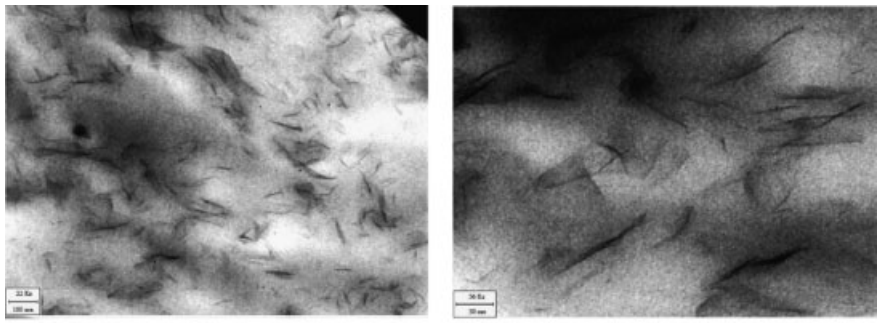

Figure 5.
TEM micrographs of normal section of 3PAextr hybrid increasing the magnification levels from (a) to (b).

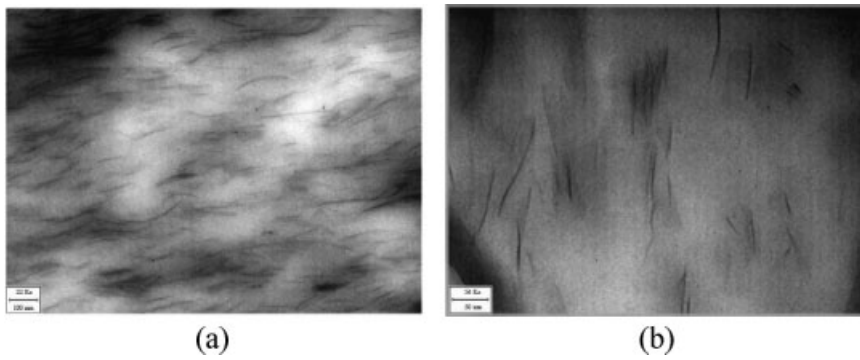

Figure 6.
TEM micrographs of normal section of 3PA0 hybrid increasing the magnification levels from (a) to (b).

γ-phase composed of plated sheets of twisted parallel chains.

The crystal structure of polyamide-6 and polyamide-6/clay fibers on drawing investigated by means of DSC measurements.

The first heating DSC traces of polyamide-6 matrix and nanocomposite systems at different silicate loadings are compared at DR = 0 (Figure 7-a) and at DR = 18 (Figure 7-b).

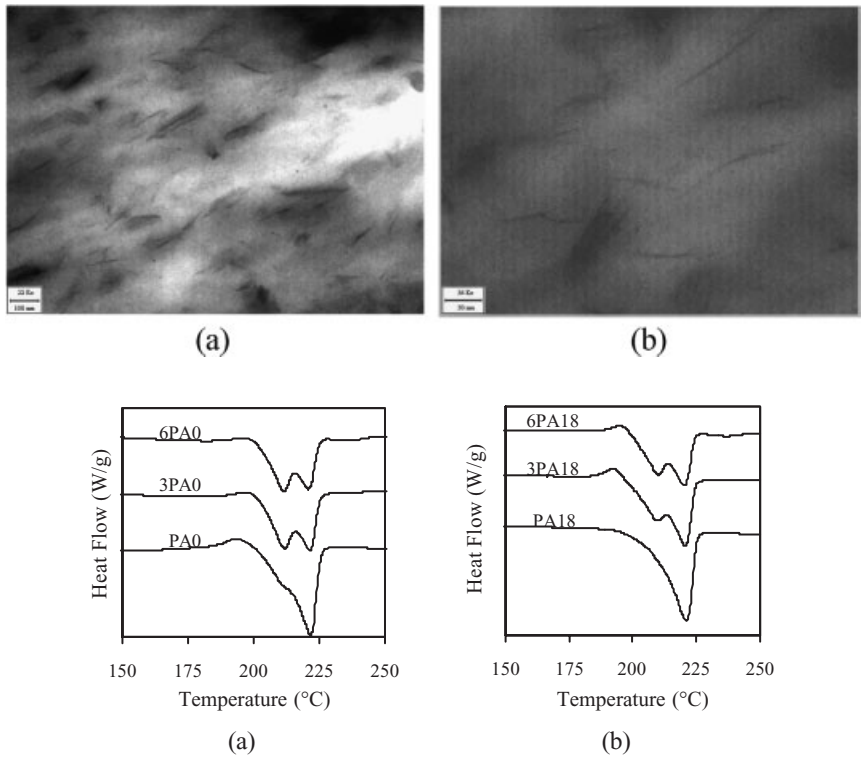

Figure 7.
TEM micrographs of normal section of 3PA18 hybrid increasing the magnification levels from (a) to (b). First heating DSC thermograms of the neat matrix and nanocomposite fibers at (a) DR = 0 and (b) DR = 18.

Analyzing the thermograms of the neat matrix (PA0 and PA18) reported in Figure 7a-b it can be observed that as increasing draw ratio only the α-crystal form, evidenced by a melting peak at 221 °C, is present as consequence of $\gamma \rightarrow \alpha$ transition promoted by stretching. This would be in agreement with the results of several authors[22,23] who demonstrated that during the drawing of polyamide-6 fibers there is an apparent transition from γ-phase crystals to α-phase crystals. In particular, Samon and Schultz[24] verified that a part of the observed γ to α-form conversion results from destruction of the γ-phase and the production of the α-phase from the amorphous fraction of polymer.

At any draw ratio, instead, all the hybrid fibers show (Figure 7a-b) a double melting peak: one at 221 °C, corresponding to the α crystal form, and the second at 210 °C related to the presence of the γ-form stabilized by the silicate. In fact, some studies about $\gamma \rightarrow \alpha$ crystalline transition of polyamide-6 based nanocomposites prior to melting[25–27] have demonstrated that the presence of silicate layers affects the phase structure of hybrid systems stabilizing a dominant γ-crystal phase. This stabilizing effect of silicate has been attributed to the polymer-aluminosilicate interactions: the layers affect the amount and the type of crystalline phase because they restrict the mobility of molecular chains due to both strongly confined spaces between layers and chemical bonds with the clay surface.

In order to evidence the effect of drawing on the crystal forms in the hybrids, in Figure 8 the first heating DSC scans for the 3wt% nanocomposite fibers are reported at different draw ratios. It can be noticed that at high draw ratios the temperature peak at 210 °C, relative to the γ-form, becomes less evident respect to the higher melting peak (221 °C), relative to the α-form. Similar trend was also observed by Yoon et al.[28]

Anyway, since the melting enthalpy values of the polymer remain almost constant, no significant changes are measured in terms of crystallinity degree of polyamide-6 and hybrid fibers at any silicate loading and draw ratio.

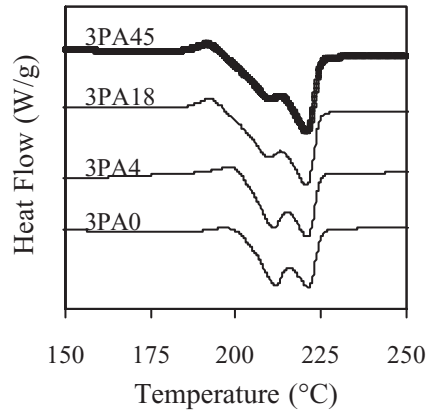

Figure 8.
First heating DSC thermograms of 3wt% nanocomposite fibers at different draw ratio (DR = 0, 4, 18, 45).

In Figure 8 it can be also observed the presence of a small endothermic peak (just before the double melting peak) only for the stretched fibers. This peak probably corresponds to the thermal induced crystallization of the polymer amorphous regions (ordered by drawing) in the most stable α-form.

Further investigations, using modulated DSC and X-Ray analysis, are in progress in order to study in more detail the crystalline structure of nanocomposite fibers upon stretching, which most likely results from a balance of two opposite effects: the first related to the silicate which stabilizes the γ form and the second due to drawing which promotes $\gamma \rightarrow \alpha$ transition.

Tensile modulus of the fibers were also investigated with the aim of correlating them to the nanostructure.

Table 2 reports Young's modulus values and its percentage increments with respect to the correspondent undrawn sample for the neat matrix and the hybrid fibers at different draw ratios.

The presence of silicate leads to substantial improvements in stiffness of the polyamide-6 matrix for both clay concentrations and at any draw ratio. However,

Table 2.
Young's modulus and its percentage increment respect to the correspondent undrawn sample for PA matrix and nanocomposite hybrids.

	PA		PA/C30B 3wt%		PA/C30B 6wt%	
Draw ratio	Young's modulus (MPa)	Percentage increment	Young's modulus (MPa)	Percentage increment	Young's modulus (MPa)	Percentage increment
0	1040 ± 90	–	1900 ± 100	–	2000 ± 100	–
4	1400 ± 100	34%	2050 ± 150	6%	2300 ± 400	15%
18	3900 ± 600	274%	4600 ± 600	137%	5700 ± 300	183%
45	4200 ± 700	306%	5300 ± 500	176%	–	–

the percentage increment of modulus with increasing the draw ratio is higher for the neat polyamide when compared to the nanocomposites. This result is probably ascribed to the increasing amount of the α-form in the neat matrix upon drawing,[24] which enhances stiffness and tensile strength of the matrix. On the other hand, the amount of crystal forms strongly affects the global tensile stress-strain behavior of the different fibers. Preliminary tests on the fibers at high draw ratios have shown a strain hardening behavior for the only neat matrix, probably due to the presence of α-crystal form.

Conclusions

In this work the elongational rheological characterization of polyamide-6 based nanocomposites, prepared by melt compounding, was realized by converging flow method and fiber spinning technique.

Steady-shear tests at high shear rates, performed with capillary rheometer, indicate reduction of shear viscosity and an increasing of extentional viscosity with the addition of the silicate. On the other hand, fiber spinning measurements show that the draw-down force of the samples increases with the silicate loading, while the breaking draw ratio decreases with the clay concentration.

During the spinning tests, fibers of neat matrix and hybrids were collected at different draw ratios in order to study the effect of uniaxial drawing on morphology (silicate dispersion and exfoliation, orientation of the layered silicate and crystallites, matrix crystalline polymorphism) of nanocomposites.

By TEM images of the hybrid fibers an enhanced degree of exfoliation of the filler upon drawing was noted. The crystalline structure of polyamide-6 and polyamide-6/clay fibers on drawing was investigated by means of DSC measurements. Two opposite effects, related to filler and draw ratio were observed: the silicate layers stabilize the γ form and the drawing promotes the α crystal phase.

The performances of the resulting nanocomposite fibers were analyzed in terms of tensile mechanical properties. In particular, the presence of silicate leads to stiffness improvement at any draw ratio. Moreover, at higher draw ratios a strain hardening behavior was observed only for the unfilled system, probably ascribed to the increasing amount of the α-form in the neat matrix upon drawing, which enhances stiffness and tensile strength.

[1] T. J. Pinnavaia, G. W. Beall, editors. *Polymer-Layered Silicate Nanocomposites*, John Wiley & Sons Ltd., NY **2001**.
[2] P. C. LeBaron, Z. Wang, T.J. Pinnavaia, *Appl. Clay Sci.* **1999**, *15*, 11.
[3] J. W. Cho, D. R. Paul, *Polymer* **2001**, *42*, 1083.
[4] L. A. Utracki, J. Lyngaae- Jørgensen, *Rheol. Acta* **2002**, *41*, 394.
[5] S. Sinha Ray, M. Okamoto, *Prog. Polym. Sci.* **2003**, *28*, 1539.
[6] R. Wagener, T. J. G. Reisinger, *Polymer* **2003**, *44*, 7513.
[7] M. Okamoto, P. Maiti, T. Kotaka, N. Hasegawa, A. Usuki, *Nano Lett.* **2001**, *1*, 295.
[8] K.W. Wang, M. Xu, Y. S. Choi, I. J. Chung, *Polym. Bull.* **2001**, *46*, 499.

[9] T. D. Fornes, D. R. Paul, *Polymer* **2003**, *44*, 3945.
[10] L. Incarnato, P. Scarfato, G.M. Russo, L. Di Maio, P. Iannelli, D. Acierno, *Polymer* **2003**, *44*, 4625.
[11] L. Incarnato, P. Scarfato, L. Scatteia, D. Acierno, *Polymer* **2004**, *45*, 3487.
[12] G. M. Russo, G. P. Simon, L. Incarnato, *Macromulecules* **2006**, *39*, 3855.
[13] E. P. Giannelis, R. Krishnamoorti, *Macromulecules* **1997**, *30*, 4097.
[14] B. Hoffmann, C. Dietrich, R. Thomann, C. Friedrich, R. Mülhaupt, *Macromol. Rapid Commun.* **2000**, *21*, 57.
[15] J. M. Dealy, K. F. Wissbrum, *Melt rheology and its role in plastics processing*. Dordrecht Kluwer Academic Publishers, **1999**.
[16] F. N. Cogswell, *Polym. Eng. Sci.* **1972**, 12 No 1, 64.
[17] P. Micic, and S. N. Bhattacharya, *Polymer International* **2000**, *49*, 1580–1589.
[18] F. J. Medellin-Rodriguez, C. Burger, B. S. Hsiao, B. Chu, R. Vaia, S. Phillips, *Polymer* **2001**, *42*, 9015
[19] A. Bafna, G. Beaucage, F. Mirabella, S. Mehta, *Polymer* **2003**, *44*, 1103
[20] S. Pavlikova, R. Thomann, P. Reichert, R. Mülhaupt, A. Marcinčin, E. Borsig, *J. Appl. Polym. Sci.* **2003**, *89*, 604
[21] V. Pasanovic_Zujo, R. K. Gupta, S. N. Bhattacharya, *Rheol. Acta* **2004**, *43*, 99.
[22] R. Prasad, V. Pasanovic_Zujo, R. K. Gupta, F. Cser, S. N. Bhattacharya, *Polym. Eng. Sci* **2004**, *44*, 1220
[23] T. D. Fornes, P. J. Yoon, H. Keskkula, D. R. Paul, *Polymer* **2002**, *43*, 2121
[24] J. M. Samon, J. M. Schultz, B. S. Hsiao, *Polymer* **2000**, *41*, 2169
[25] T. M. Wu, C. S. Liao, *Macromol. Chem. Phys.* **2000**, *201*, 2820
[26] T. M. Wu, E. C. Chen, C. S. Liao, *Polym. Eng. Sci.* **2002**, *42*, 1141
[27] E. Devaux, S. Boubigot, A. Achari, *J. Appl. Polym. Sci.*, **2002**, *86*, 2423
[28] K. Yoon, M. B. Polk, B. G. Min, D.A. Schiraldi, *Polym. Int.* **2004**, *53*, 2072

